

Fuzzy-based estimation of reference flux, reference torque and sector rotation for performance improvement of DTC-IM drive

Sampath Kumar Subramaniam, Joseph Xavier Rayappan & Balamurugan Sukumar

To cite this article: Sampath Kumar Subramaniam, Joseph Xavier Rayappan & Balamurugan Sukumar (2022) Fuzzy-based estimation of reference flux, reference torque and sector rotation for performance improvement of DTC-IM drive, *Automatika*, 63:3, 440-453, DOI: [10.1080/00051144.2022.2051966](https://doi.org/10.1080/00051144.2022.2051966)

To link to this article: <https://doi.org/10.1080/00051144.2022.2051966>



© 2022 The Author(s). Published by Informa UK Limited, trading as Taylor & Francis Group.



Published online: 17 Mar 2022.



Submit your article to this journal [↗](#)



Article views: 435



View related articles [↗](#)



View Crossmark data [↗](#)



Fuzzy-based estimation of reference flux, reference torque and sector rotation for performance improvement of DTC-IM drive

Sampath Kumar Subramaniam^a, Joseph Xavier Rayappan^b and Balamurugan Sukumar^a

^aDepartment of Electrical and Electronics Engineering, Amrita School of Engineering - Coimbatore, Amrita Vishwa Vidyapeetham, India;

^bAkshya College of Engineering and Technology, Coimbatore, India

ABSTRACT

In this study, the fuzzy-based reference flux estimator (RFE), reference torque estimator (RTE) and sector rotation strategy called fuzzy logic estimator are proposed to direct torque control of induction motor (DTC-IM) drive for performance improvement. The basic DTC-IM drive with conventional RFE, RTE and sector division causes large torque ripple, variable switching frequency and uneven voltage vector contribution in stator flux. The torque and speed responses of the proposed system are investigated with load variations. The simulation results of the proposed DTC-IM drive are compared with the basic DTC-IM drive. The assessment of the proposed system shows improved performance. A hardware is developed using Xilinx Spartan-6XC6SLX45-Field Programmable Gate Array (FPGA) Kit for experimental verification of the results. Moreover, sinusoidal pulse width modulation and space vector pulse width modulation techniques are applied to reduce the torque ripples. The performance of the drive is investigated for various speed ranges. The comparison of the simulated and experimental results proves that the proposed fuzzy-based DTC-IM drive provides better performance than the basic DTC-IM drive.

ARTICLE HISTORY

Received 30 September 2020
Accepted 8 March 2022

KEYWORDS

Direct torque control; fuzzy logic; adaptive; sector; reference flux; sinusoidal pulse width modulation; space vector pulse width modulation

1. Introduction

In advanced motor drive applications, direct torque control of induction motor (DTC-IM) drives have been used widely owing to their instantaneous torque and flux control with simple structure. The DTC drive system is identified for its robustness and dependency on motor parameter variations [1,2]. However, DTC control scheme uses hysteresis comparators for torque and flux control which causes variable switching frequency and torque ripple. Hence, it requires high sampling rate for experimental validation. DTC scheme applies voltage vectors to IM based on the switching table which is developed based on hysteresis comparators output and stator flux angle. The instantaneous requirements of variation in stator flux and torque are accomplished by the switching table. The stator flux plot has been separated into six equal sectors with respect to stator flux angle, and DTC scheme is developed using the induction machine model [3,4].

The literature survey indicates that the stator flux control and torque control of DTC-IM are enhanced by employing soft computing control strategies like fuzzy logic controller (FLC), neural networks and genetic algorithm [5]. The bandwidth of the torque hysteresis comparator is adjusted using FLC to reduce torque and flux ripples [6]. The virtual voltage vectors as well as model predictive control methods are proposed for improving the performance of DTC [7,8]. Using

intermediate voltage vectors by synthesizing the conventional full voltage vectors, an altered switching table was proposed for preventing the demagnetization of stator flux in DTC. However, the synthesizing of voltage vectors and computation of flux and torque ripples becomes complex [9].

The reference value of stator flux is significantly influencing the torque ripples in DTC. Nominal value of stator flux is not suitable for all load variations. Hence, the reference flux is optimized as a function of torque to reduce the torque ripple [10]. In Ref. [11], fuzzy logic is used as stator flux optimizer for self-regulating the value of reference flux in DTC. However, the fuzzy membership functions are asymmetric across the operating range. Some ranges do not come under any membership functions. The reference flux is optimized by torque variations with the aid of fuzzy logic, Artificial Neural Network (ANN) and Adaptive Neuro Fuzzy Inference System [12]. The symmetrical membership functions are used for fuzzy logic in Ref. [12]. On the other hand, the results are investigated only through simulation [11,12].

The DTC scheme uses Proportional Integral (PI) controller in speed control loop to produce the reference torque by tracking speed error as input. The fine tuning of PI controller helps to improve the dynamic speed response of the DTC-IM drive [12,13]. Soft computing techniques are used to tune the PI

controller [14]. The fuzzy gain scheduling (FGS) decides the gain values of the PI controller through online tracking of the speed error [12–14]. The input membership functions are seven and output membership functions are only two, so that optimum speed control is not attained [13]. Seven membership functions are used for input and output of FGS [12,14]. However, the results are validated only through simulation [12–14].

In basic DTC scheme, the stator flux drooping at low speeds near flux sector boundaries have been investigated [15]. By rotating the sectors of the stator flux plot based on the states of torque and flux hysteresis comparators output, the performance of the DTC system is improved. Gated sector rotation in DTC is introduced in Ref. [15]. The sector rotation angle has to modify every time whenever the system condition changes. The decoupling of the stator flux amplitude and angle for selecting reference stator voltage vectors to avoid the flux droop during sector transition is discussed in Ref. [16].

The flux and torque hysteresis band magnitudes are varied and the effect of variation on the dynamic performance of DTC-IM drive is investigated [17]. The existing DTC techniques for inverter fed IM and permanent magnet synchronous motors together with soft computing controllers are presented [18]. The performance of the drive in low speed regions can be improved by the model reference adaptive system-based direct flux magnitude estimation technique [19]. Conventional PI controller is made adaptive to improve the reference torque in DTC [20,21]. A comparative study between DTC based on fuzzy and DTC based on sinusoidal pulse width modulation (SPWM) is performed [22]. The variation of stator resistance at low speeds in DTC-IM drive is investigated [23].

This paper contributes to DTC majorly by

- (i) Proposing a DTC scheme with fuzzy-based reference flux estimator (RFE), FGS-based PI speed controller, and fuzzy-based sector rotation.
- (ii) The fuzzy-based sector rotation scheme has not been tried by any other researchers.
- (iii) The proposed fuzzy DTC scheme and basic DTC scheme are developed in hardware setup. The experimental results are correlated with simulation results.
- (iv) The developed DTC scheme is validated by changing the reference speed to medium and low speed ranges to prove the high performance.
- (v) SPWM and space vector pulse width modulation (SVPWM) are applied to improve the performance of the DTC-IM drive.

All the three fuzzy logic estimator (FLE) are developed to operate together adaptively according to the instantaneous system conditions. Hence, the proposed

fuzzy DTC-IM drive will be better than the basic DTC-IM drive for reducing torque ripples and adaptive speed control.

In this paper, Section 2 describes the basic DTC with fixed angle sector rotation. Section 3 discusses about SPWM, SVPWM as well as the three FLE, namely, fuzzy-based RFE, fuzzy-based reference torque estimator (RTE) (FGS-based PI speed controller) and fuzzy-based sector rotation. In Section 4, the development of the experimental setup for the basic DTC and fuzzy DTC is described in detail. Section 5 investigates the simulation and experimental results as well as the performance indices of the basic DTC, SPWM-DTC, SVPWM-DTC and proposed fuzzy DTC. The proposed schemes are validated by various reference speeds like nominal, medium and low speeds to prove the high performance. In Section 6, it is found that the proposed fuzzy DTC is performing superior to the basic DTC based on simulation and experimental results.

2. DTC with sector rotation

The block diagram of basic DTC-IM drive is presented in Figure 1. The IM of DTC is operated by stator flux and torque hysteresis comparators. The inverter switching states are selected by a predefined look-up table [1]. The stator flux of the DTC-IM drive can be defined using voltage space vector (U_s) in Equation (1) by ignoring the stator resistance (R_s) as [2,3]

$$\Delta\Psi = U_s * \Delta t. \quad (1)$$

The stator flux plot is separated as six sectors as given in Figure 2. The stator flux hysteresis comparator ($d\Psi_s$), torque hysteresis comparator output (dT) and the sector number $\alpha[i]$ of stator flux angle (α) are used for selecting the switching voltage vectors. The look-up table is furnished in Table 1 [4].

The drawback in basic DTC is that while the stator flux vector changes from beginning of a sector to the end, the effect of the voltage vectors is not the same throughout the sector as shown in Figure 3. When the stator flux has to be improved and torque has to be reduced in sector I, the voltage vector U6 has to be applied based on Table 1. The activeness variation of U6 at the beginning and end of the sector I is shown in Figure 3(a). In the same way, when U5 is applied, activeness variation is given in Figure 3(b).

It shows that at the beginning of sector I, the look-up table gives U6. However, U5 is also compatible at the beginning of sector I, suggested by the look-up table for sector VI. In the same way, at the end of sector I, instead of U6 the voltage vector U1 is compatible, suggested by the look-up table for sector II. The change of stator flux decides the effectiveness of voltage vector to meet the desired output. If the sectors of stator flux plot based on stator flux angle (α) are slightly rotated by an angle, then the performance improvement in the DTC scheme

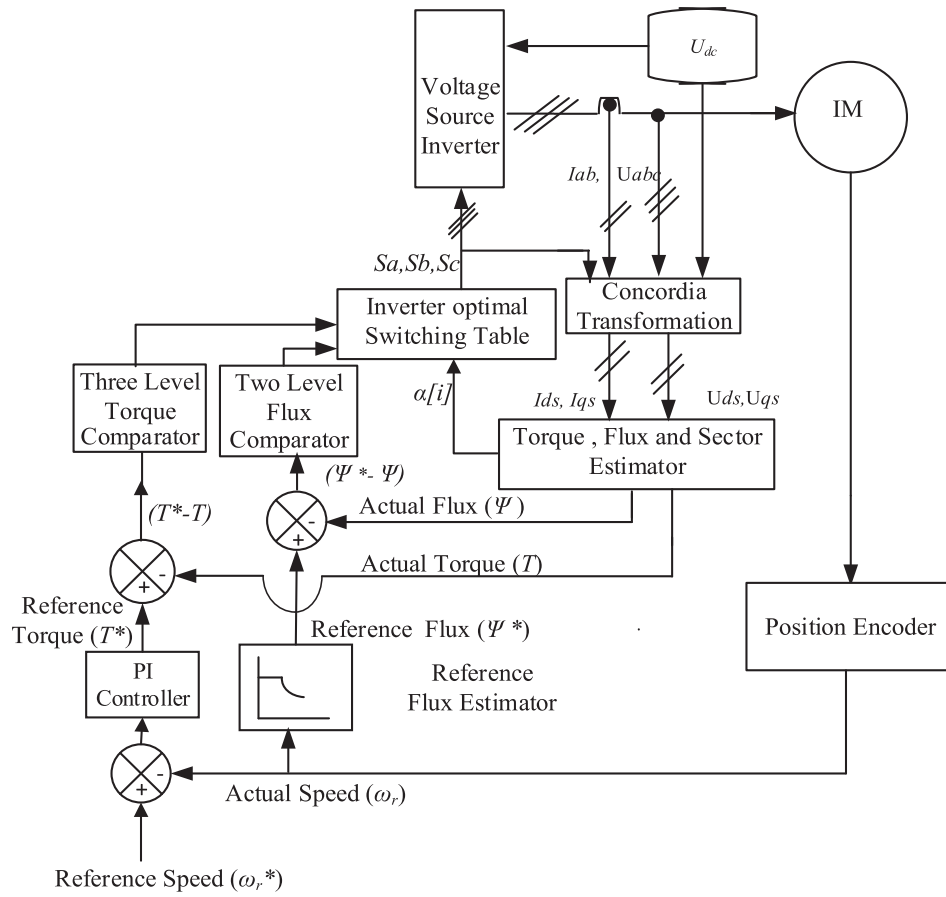


Figure 1. Block diagram of the DTC-IM drive.

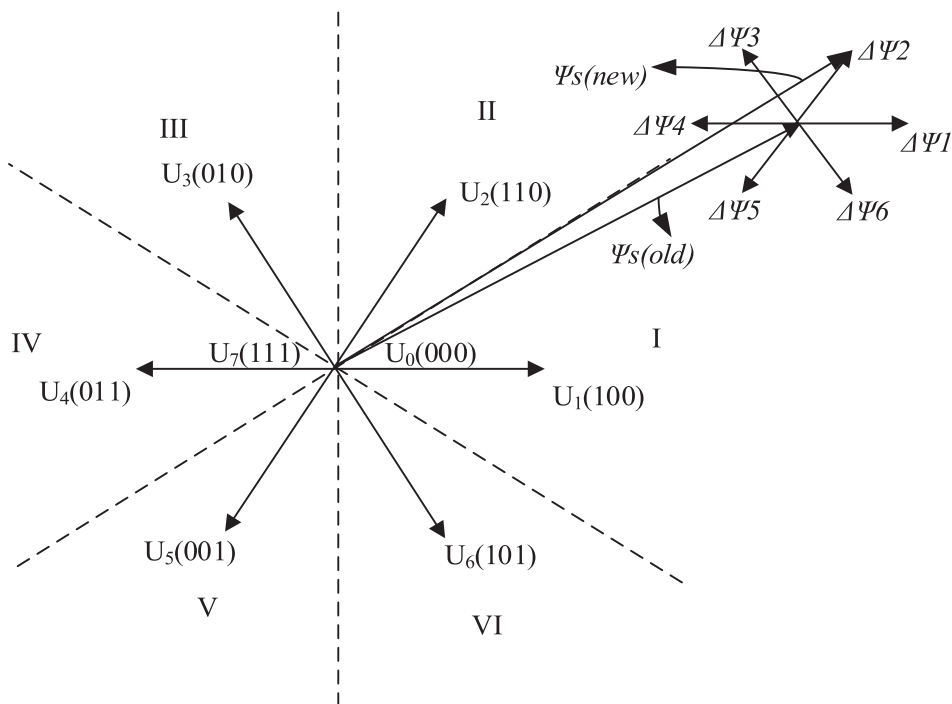


Figure 2. Stator flux plot and voltage vectors in conventional DTC.

Table 1. Look-up table for DTC.

$d\Psi_s$	dT	Sector number					
		I	II	III	IV	V	VI
1	1	U2	U3	U4	U5	U6	U1
1	0	U0	U7	U0	U7	U0	U7
1	-1	U6	U1	U2	U3	U4	U5
0	1	U3	U4	U5	U6	U1	U2
0	0	U7	U0	U7	U0	U7	U0
0	-1	U5	U6	U1	U2	U3	U4

can be achieved [15]. The proposed sector rotation is implemented using Equations (2) and (3) for modified stator flux angle (α_m):

$$\alpha_m = \alpha + \Delta\alpha, \quad (2)$$

$$\Delta\alpha = \alpha_{rot} d\Psi_s dT, \quad (3)$$

where α_{rot} is the angle by which the sectors are shifted from original position, $d\Psi_s$ and dT are the outputs from flux and torque hysteresis comparators. In this paper, in basic DTC, sector rotation is performed at a particular angle to improve the performance.

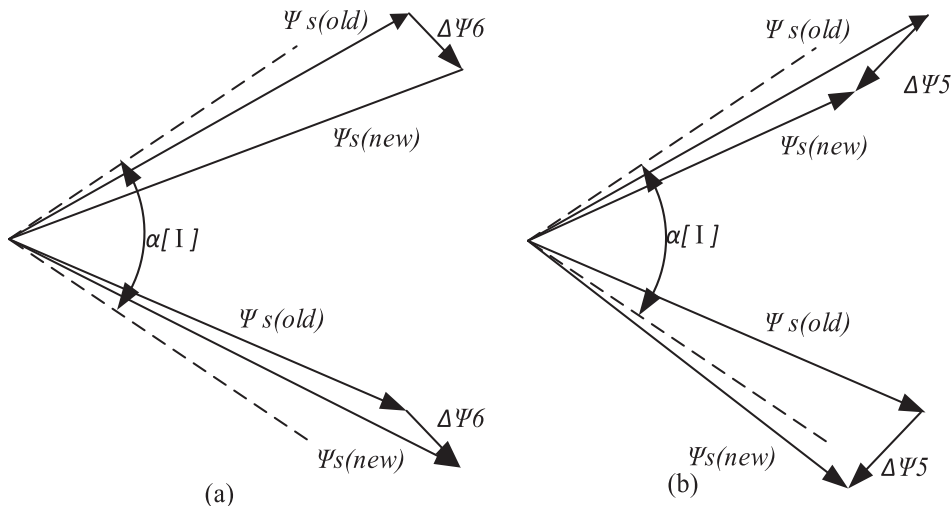
3. SPWM, SVPWM and fuzzy in DTC

The SPWM, SVPWM and fuzzy logic are applied in this paper to reduce the ripples in torque and better speed control for DTC-IM drive.

3.1. SPWM and SVPWM-based DTC

The basic induction machine (Equation (1)) clearly depicts that the stator flux variation is proportional to the applied voltage vector direction and the time period Δt . The developed electromagnetic torque (T_e) is also dependent on the stator flux [1] as per Equation (4). The block diagram of the DTC-SPWM/SVPWM strategies is shown in Figure 4.

$$T_e = \Psi_s X I_s. \quad (4)$$

**Figure 3.** Uneven voltage vector contribution in sector I. (a) For voltage vector U6 and (b) for voltage vector U5.

The torque, flux hysteresis comparators as well as the look-up table are replaced by PI controllers and SPWM/SVPWM module. The PI controllers are used to decide the required voltage vectors.

In SPWM, the outputs of the PI controllers are used to construct the reference sinusoidal signals (dq-abc). The constructed reference signals are compared with triangular wave carrier signal to determine the switching states of inverter.

The applied voltage vector and its duration affect the torque and flux. The applied voltage vectors are synthesized using predetermined time intervals by SVPWM technique. Each cycle period is subdivided by computing the voltage space vectors required for torque and flux errors sampled from previous state.

3.2. Fuzzy-based estimators for DTC-IM drive

Mamdani-type fuzzy logics are developed for DTC-IM drive. The reference flux value (Ψ^*), gain values for the PI speed controller and the sector rotation angle (α_{rot}) are decided by the fuzzy logic in this paper.

3.2.1. Fuzzy-based reference flux estimation

The fuzzy logic is used to fine-tune the reference flux (Ψ^*) value estimated by the conventional RFE [11]. In normal DTC operation, the standard RFE gives the reference flux value derived from whether the motor operating at constant flux region or field weakening region [10]. If the flux level is adjusted in proportion to the load, the energy consumed by the drive can be reduced [10–12]. The RFE output (Ψ^*) and actual flux (Ψ) are used to calculate the flux error ($\Psi^* - \Psi$) as shown in Figure 1 [1]. In real-time experimental validation, the actual flux is estimated using U_{ds} , U_{qs} , I_{ds} and I_{qs} components with the help of current and potential transducers.

By using torque error ($T^* - T$) and reference flux (Ψ^*) from conventional RFE, FLE calculates the

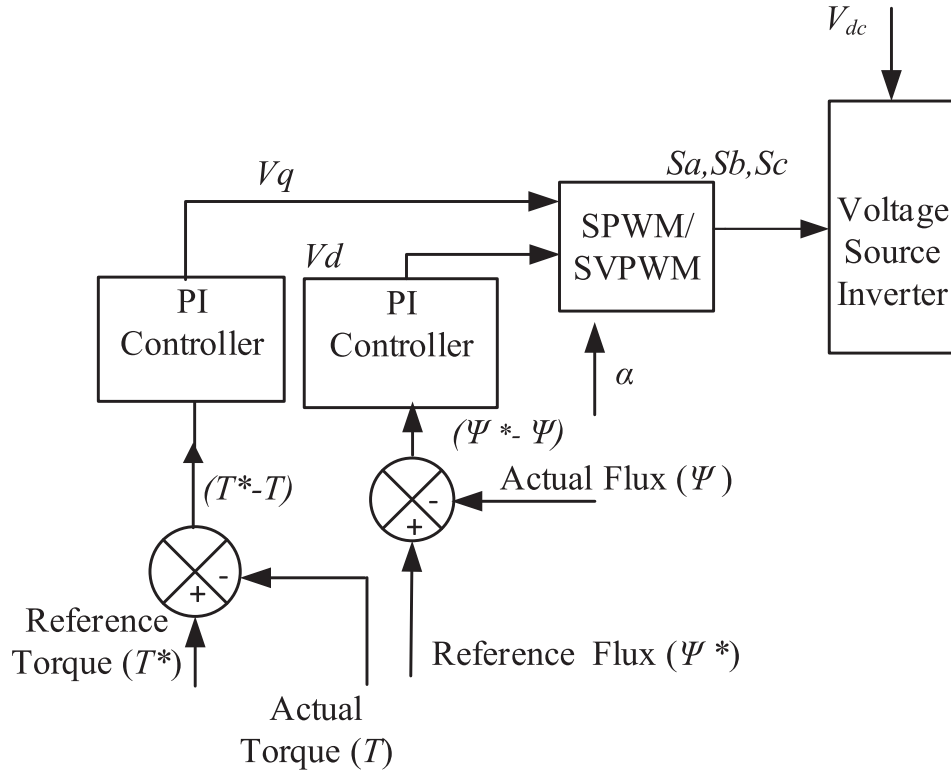


Figure 4. SPWM/SVPWM for DTC.

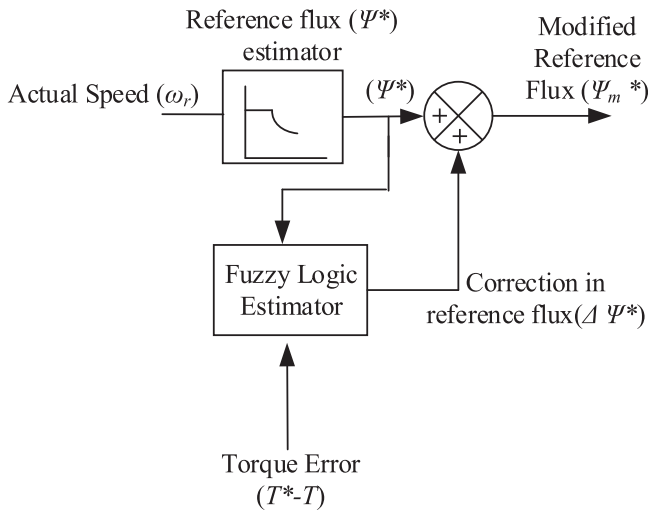


Figure 5. Fuzzy-based RFE.

correction in reference flux ($\Delta\Psi^*$) as presented in Figure 5. To reduce the torque ripple, fuzzy logic gives the correction in reference ($\Delta\Psi^*$) through approximation [11,12]. This correction in reference flux ($\Delta\Psi^*$) is added with reference flux (Ψ^*) to obtain the modified reference flux (Ψ_m^*) as per Equation (5).

$$\Psi_m^* = \Psi^* + \Delta\Psi^* \quad (5)$$

The $(T^* - T)$, Ψ^* and $\Delta\Psi^*$ are fuzzified using six {NB = negative big, NM = negative medium, N = negative, P = positive, PM = positive medium, PB = positive big}, three S = small, M = medium, B = big} and seven {NB = negative big, NM = negative

Table 2. Rule base for reference flux estimation.

$(T^* - T)$							
		NB	NM	N	P	PM	PB
Ψ^*	S	O	PM	PB	O	PM	PB
	M	NS	O	PS	NS	PM	PS
	B	NB	NM	O	NB	NM	O

medium, NS = negative small, O = zero, PS = positive small, PM = positive medium, PB = positive big} membership functions, respectively. The universe of $(T^* - T)$, Ψ^* and $\Delta\Psi^*$ are $[-100$ to $100]$, $[0$ to $1]$ and $[-0.2$ to $0.2]$, respectively.

The $(T^* - T)$ uses four trapezoidal membership functions {NB, NM, PM, PB} and two {N, P} triangular membership functions. The Ψ^* uses two trapezoidal {S, B} and one triangular {M} membership function. The $\Delta\Psi^*$ uses five triangular {NM, NS, O, PS, PM} and two trapezoidal {NB, PB} membership functions [12]. The 18 rules of the developed FLE are given in Table 2 [12].

In Ref. [11], the membership functions are distributed discontinuously and irregularly. Hence, in this paper, an attempt has been made to implement the symmetrical membership functions proposed by the authors [12] experimentally.

3.2.2. Fuzzy-based reference torque estimation

The torque ripples can be further reduced by replacing the fixed gain PI speed controllers in basic DTC to adaptive gain PI speed controllers. This is accomplished using fuzzy logic for gain scheduling. Figure 6 shows

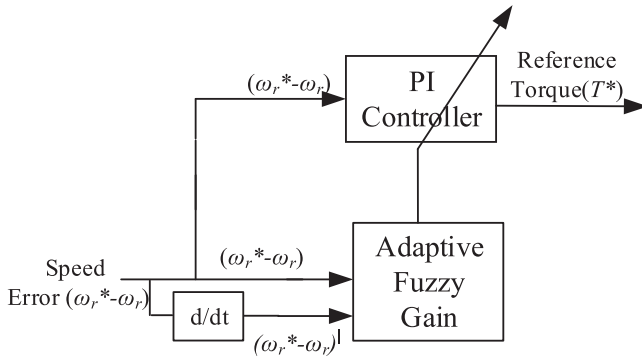


Figure 6. Block diagram of FGS tuned PI speed controller.

Table 3. Rule table for K_p and K_i .

K_{PFGS} and K_{IFGS}	$(\omega_r^* - \omega_r)$							
	XS	VS	S	M	B	VB	XB	
$(\omega_r^* - \omega_r)^1$	XS	XB	XB	XB	VB	VB	B	M
	VS	XB	VB	VB	VB	B	M	S
	S	XB	VB	B	B	M	S	VS
	M	VB	VB	B	M	S	VS	VS
	B	VB	B	M	S	S	VS	XS
	VB	B	M	S	VS	VS	VS	XS
	XB	M	S	VS	VS	XS	XS	XS

the PI speed controller with gain scheduler. The attitude is to exploit fuzzy reasoning to develop the control parameters.

In FGS, the gain values are calculated based on speed error $(\omega_r^* - \omega_r)$ and its first derivative $(\omega_r^* - \omega_r)^1$. The outputs of the FGS are K_{PFGS} and K_{IFGS} from which the gain values of speed PI controller are calculated using Equations (6) and (7). The K_{PFGS} and K_{IFGS} values are assumed with certain ranges [12,13].

$$K_p^1 = (\omega_r^* - \omega_r)K_{PFGS}, \quad (6)$$

$$K_i^1 = (\omega_r^* - \omega_r)K_{IFGS}, \quad (7)$$

where K_p^1 and K_i^1 are the optimal online tuning gain values. The input and output membership functions are of five symmetrical triangular membership functions {VS = very small, S = small, M = medium, B = big, VB = very big} and two trapezoidal membership functions {XS = extra small, XB = extra big}. The inputs, speed error $(\omega_r^* - \omega_r)$ and rate of change of speed error $(\omega_r^* - \omega_r)^1$ are normalized for 0–1 and –1 to 1, respectively. The outputs K_{PFGS} and K_{IFGS} are in between 0–100 and 0–0.75, respectively. The rule base is furnished in Table 3 [14].

Table 3 is used for load frequency control in hydro thermal system [14], whereas Table 3 is used here for adaptive speed control in DTC.

3.2.3. Fuzzy-based sector rotation

In Section 2, the sector division is rotated at a fixed angle for performance improvement [15,16], but the rotation angle has to be varied accordingly when the system condition changes. In this section, the sector

Table 4. Rule base for sector rotation.

		$(T^* - T)$		
		S	M	B
$(\Psi^* - \Psi)$	S	VH	L	VL
	M	L	M	H
	B	VL	H	VH

rotation angle is chosen using fuzzy logic for the controller to be adaptive. The direction of sector rotation depends on the outputs from torque and flux hysteresis comparators. The torque error $(T^* - T)$ and flux error $(\Psi^* - \Psi)$ values are the inputs to the respective hysteresis comparators.

Whenever the torque error $(T^* - T)$ and flux error $(\Psi^* - \Psi)$ are high, the sectors must be rotated in anti-clockwise direction. In the same way, while the torque error $(T^* - T)$ and flux error $(\Psi^* - \Psi)$ are low, the sectors must be rotated in clockwise direction. The FLE uses torque error $(T^* - T)$ and flux error $(\Psi^* - \Psi)$ as inputs. The output is the change in sector rotation angle $(\Delta\alpha)$ as shown in Figure 7. For both inputs, two trapezoidal {S = small and B = big} and one triangular {M = medium} symmetrical membership functions are used. The output of the FLE has three symmetrical triangular membership functions {H = high, M = medium, L = low} and two symmetrical trapezoidal membership functions {VH = very high and VL = very low}. The membership functions are scaled down to –1 to 1. For all the FLCs used in this paper, centroid-type defuzzification method is used. The modified stator flux angle (α_m) for sector division is calculated as shown in Equation (2). In Table 4, a systematic algorithm is followed using the torque error $(T^* - T)$ values and flux error $(\Psi^* - \Psi)$ values. If the product of torque error and flux error is greater than zero, then the sectors have to be rotated in anti-clockwise and vice versa. The linguistic values should be selected such that the maximum angle of rotation is 30°.

4. Experimental setup for basic and fuzzy DTC-IM drive

The experimental setup of the proposed fuzzy DTC-IM drive has been developed to analyse the performance. In this work, the setup is built using “Xilinx Spartan-6XC6SLX45-FPGA Kit in 7G676 package” for verification.

The FPGA program design for DTC control algorithm is performed in PC using Xilinx integral square error (ISE) project navigator (P40xd) software. The Xilinx Spartan FPGA board is interfaced to the PC through dual port to embed the control algorithm. The basic DTC and fuzzy DTC control algorithms are developed individually in the computer. Based on

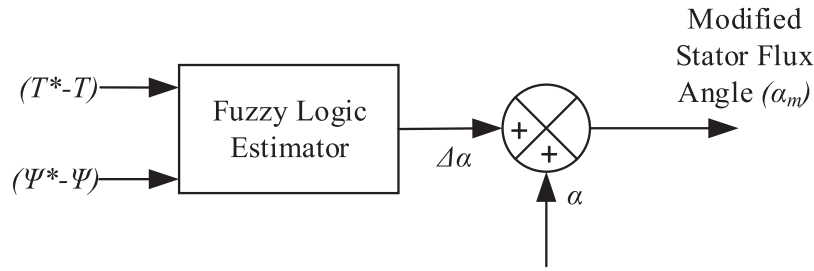


Figure 7. Fuzzy-based sector rotation.

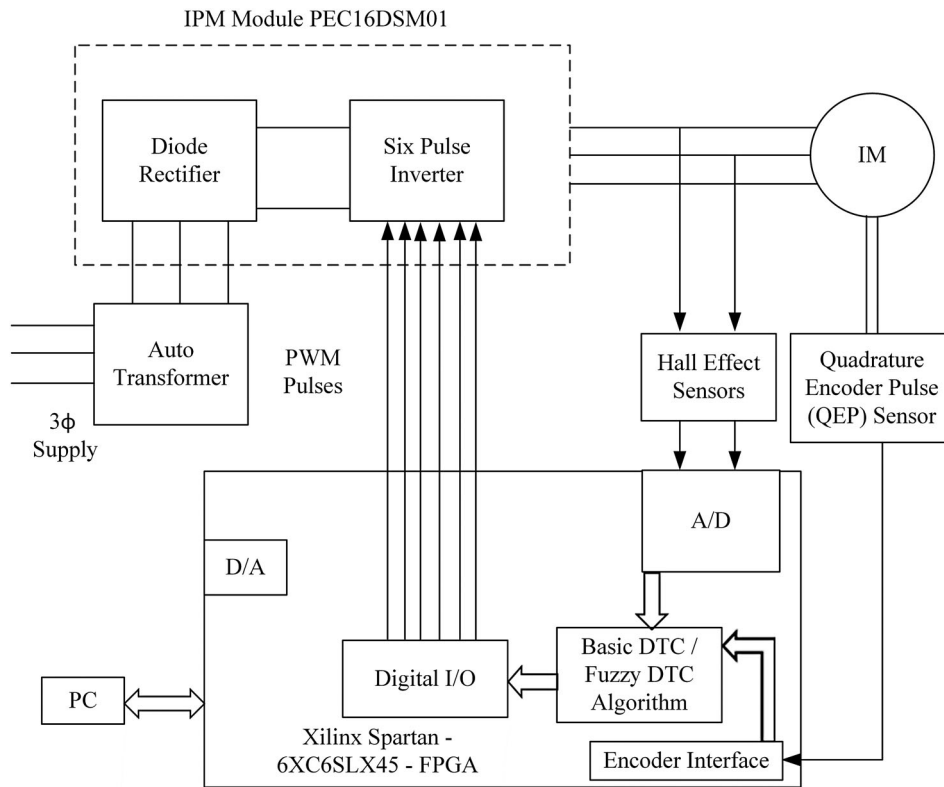


Figure 8. Schematic diagram of experimental setup for the DTC-IM drive.

the requirement, the respective algorithms are embedded. The Xilinx Spartan-6XC6SLX45 model contains 43,661 logic cell equivalents, 16 pulse width modulation (PWM) outputs and 8 capture inputs. Furthermore, it is furnished with analog to digital (A/D) converters, digital to analog (D/A) converters, serial interface and encoder interface as onboard peripherals. The clock frequency of the Xilinx Spartan-6XC6SLX45 is 20 MHz.

The schematic diagram of the developed experimental setup of DTC-IM drive is given in Figure 8. The IM with 1HP power rating is supplied by inverter with switching frequency of 10 kHz. Quadrature encoder pulse (QEP) shaft encoder with 512 pulses per revolution is used to measure the speed of the IM. The encoder output is interfaced to the FPGA using QEP signal processing card. Furthermore, the IM currents are measured by hall-effect sensors and delivered to FPGA using A/D channel.

Only two phase currents are sensed and given to FPGA. The third phase is calculated from the measured two phases. The reference speed (ω_r^*) of the IM used is 146.53 rad/s. It is possible to run the IM at 149.67 rad/s but as a safety measure, the reference speed (ω_r^*) is kept at 146.53 rad/s. The actual speed of IM is subtracted with reference speed (ω_r^*) to obtain error signal. The speed error is fed to PI controller for reference torque. The proportional (K_p) and integral (K_i) gain values of the manual tuned PI controller are 2 and 0.3, respectively. The reference flux (Ψ^*) value is based on the actual speed (ω_r) of the IM.

Based on the actual measurements from sensors and encoders, control algorithms are developed in the FPGA for basic DTC and fuzzy DTC strategies. The actual torque (T), actual flux (Ψ) and stator flux angle (α) of the IM are estimated using the reconstructed voltages and currents in the control algorithm. If the control algorithm embedded in the FPGA kit is for

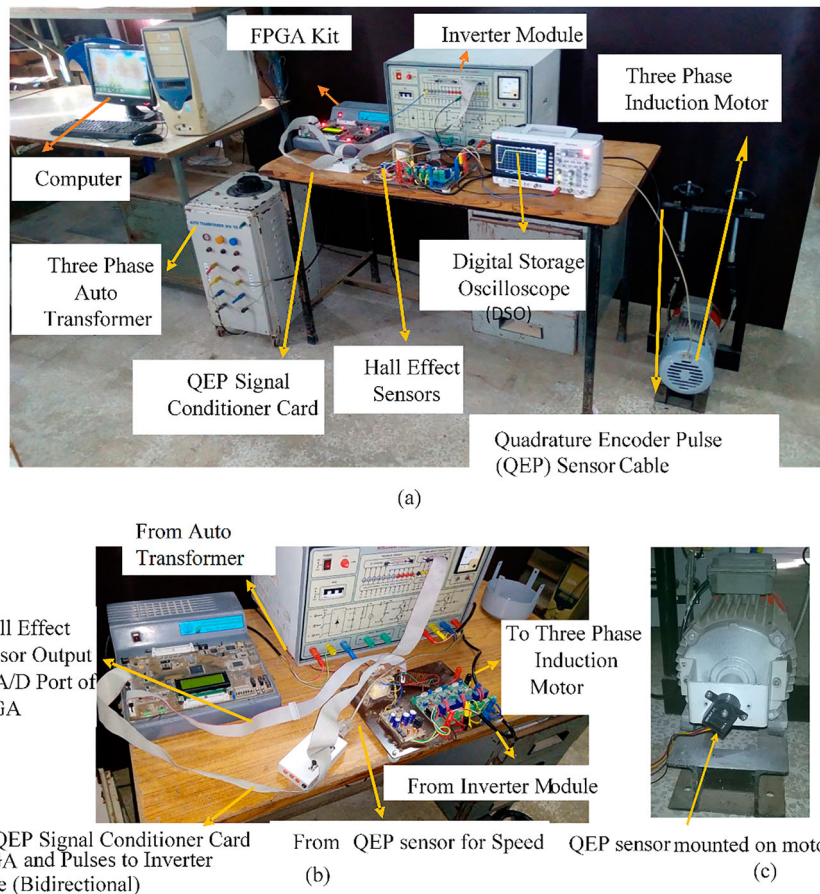


Figure 9. (a) Experimental setup for the proposed DTC-IM drive. (b) Peripheral connections of FPGA. (c) QEP sensor mounted on motor shaft.

basic DTC, then the respective PWM pulses are sent to the driver circuit of the inverter. Similarly, the PWM pulses for fuzzy DTC are also sent to the inverter by the corresponding control algorithm. Based on the inverter output, the IM performs. Hence, the individual performance of basic DTC and fuzzy DTC are measured.

The integrated power module (IPM) – PEC16DSM01 – is used as an inverter. The IPM is supplied by three-phase auto transformer, and DC link voltage of the inverter is maintained at 400 V. The timings of the load variations are followed based on Ref. [6]. The motor is loaded by direct step loading at 6, 12 and 16 s with full load (5 N m), half load (2.5 N m) and no load (0 N m), respectively. The torque output is measured from FPGA in terms of voltages from D/A ports with a scaling factor of 1.03 for basic and 1.42 for the fuzzy DTC system. The FPGA output of the speed responses are obtained in terms of voltages with a scaling factor of 25.64 for basic DTC and 38.46 for fuzzy DTC. In Section 5, using scaling factors, the simulation and experimental responses are shown in the same scale for better understanding. The developed experimental setup, peripheral connections of FPGA and shaft encoder are shown in Figure 9. The responses are perceived with a digital storage oscilloscope (DSO) having 70 MHz bandwidth and 2 GSa/s sampling rate and the

data saved as Microsoft Excel comma separated values (MECSVs) file.

5. Validation of simulation and experimental responses of DTC

The simulation model is created with MATLAB/Simulink[®] environment for basic DTC and fuzzy DTC. The experimental setup of the DTC-IM drive is developed as explained in the previous section for validation. The simulation and experimental results are compared for different loading conditions. The parameters furnished in Appendix used for simulation are obtained from actual experimental setup. This paper mainly focusses on torque ripples and speed control at various speed ranges for varying loads than voltages and currents.

5.1. Comparison of torque responses

Figure 10 compares the torque responses of the DTC-IM drive for basic DTC and fuzzy DTC. The simulation and experimental responses are compared for the load variations. It is perceived that the torque ripples are less in fuzzy DTC than basic DTC in both simulation and experiment. The results clearly indicate that the

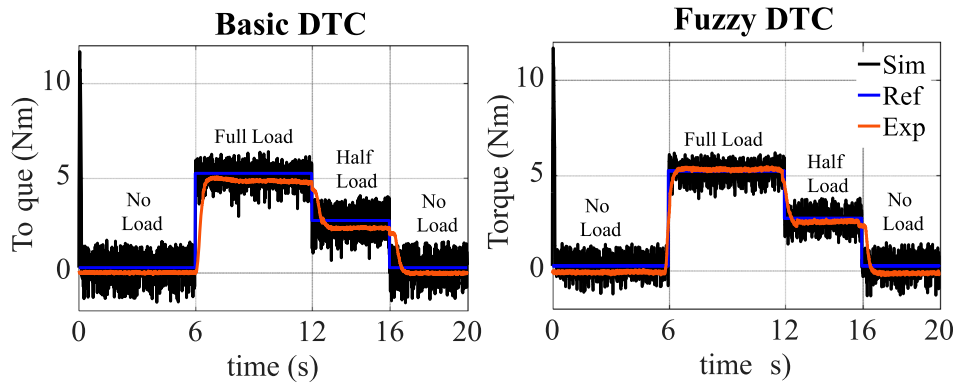


Figure 10. Torque responses of basic and fuzzy DTC schemes.

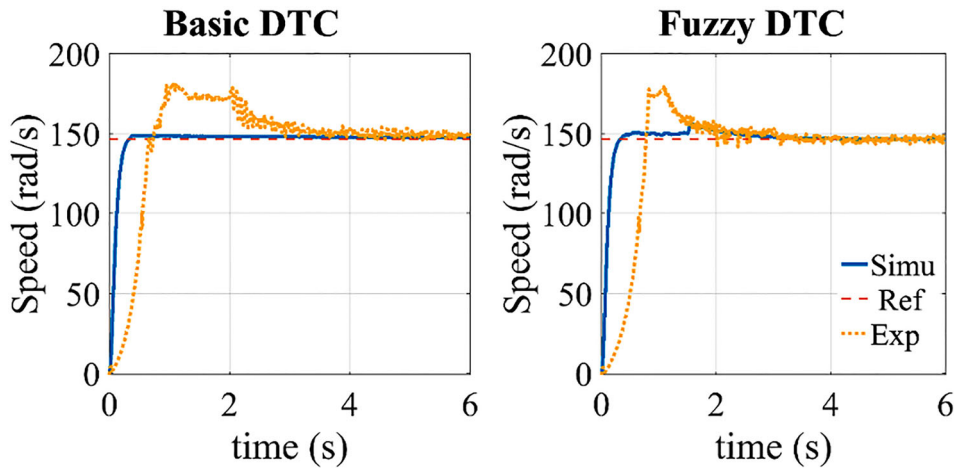


Figure 11. Speed responses of basic and fuzzy DTC schemes during starting.

reference torque is followed closely in fuzzy DTC than basic DTC.

5.2. Comparison of speed responses

Like torque response, the speed response variations are also compared for the basic DTC with the proposed fuzzy DTC system. The starting speed characteristics are given in Figure 11 for basic DTC as well as fuzzy DTC. At starting, the speed characteristics of basic DTC has less rise time with no overshoot and quick settling time than fuzzy DTC in simulation. Similar behaviour is reflected in experiment for rise time, but the overshoot is less and the settling time is compatible. The FLE takes a small time deviation to get settled in the system. Since no soft computing estimators are involved in basic DTC, it takes less rise time. The reference speed (ω_r^*) is followed closely in fuzzy DTC than basic DTC. The speed responses of the proposed fuzzy DTC-IM drive are related with basic DTC-IM drive for full load, half load and no load variations as presented in Figure 12. The simulation responses indicate that the drop in speed for the same load is more in basic DTC than fuzzy DTC. When the load is reduced, the speed is recovered nearer to the reference speed (ω_r^*) in fuzzy DTC than basic DTC. The experimental responses prove that

the fuzzy DTC is superior to basic DTC for all load variations.

5.3. Comparison of speed and torque responses at medium and low speeds

In high performance drives like DTC, the drive should be able to perform even at medium and low speed ranges. Hence, the developed control strategies are verified for medium (146.53×0.4 rad/s) and low speed ranges (146.53×0.06 rad/s).

It is perceived that the torque ripples are more in the proposed DTC schemes, and to validate the performance, SPWM and SVPWM techniques are introduced in DTC [17–22]. The speed responses of the SPWM- and SVPWM-based DTC are given in Figure 13 for nominal, medium and low reference speeds. It is seen that SPWM performs at nominal and medium speed ranges but for low speed range, the performance of SPWM is not satisfactory. The SVPWM performs at nominal speed range but for medium and low reference speeds, the performances are not satisfactory. In nominal speed range, the SVPWM performs better than SPWM.

The DTC-IM drive is independent of all the machine parameters except stator resistance (R_s) of the IM. At

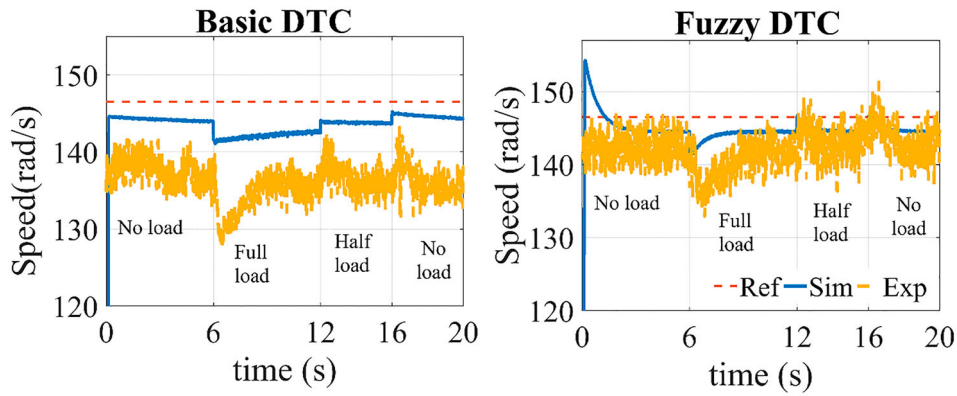


Figure 12. Steady-state speed responses of basic and fuzzy DTC schemes: full load, half load and no load.

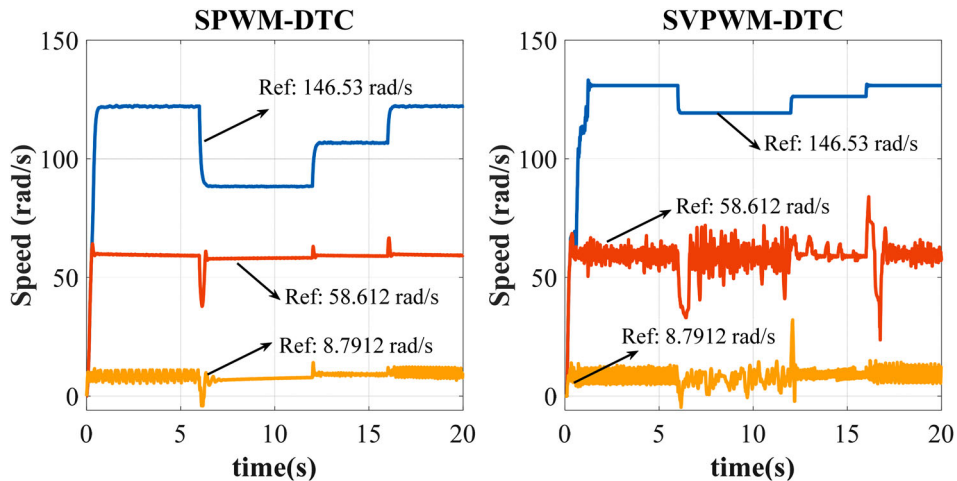


Figure 13. Speed responses of SPWM-DTC and SVPWM-DTC schemes for a speed reference of 146.53, 51.612 and 8.7912 rad/s.

nominal speed range, stator resistance drop ($I_s R_s$) is negligible when compared to input voltage. In medium and low speed ranges, the input voltage becomes proportionately less. Hence, the value of stator resistance drop ($I_s R_s$) is acute while related to input voltage as shown in Equation (8). Moreover, during the operation of the drive, the stator resistance (R_s) changes due to temperature. The change in stator resistance (R_s) causes the change in stator current (I_s). It causes incorrect stator flux estimation, consequently the developed electromagnetic torque (T_e) as in Equation (4) and position of stator flux [23]. When the developed electromagnetic torque (T_e) is not proper and load torque remains same, the speed control becomes difficult [12]. Hence, no major improvements are observed in speed responses at medium and low speed ranges.

$$\Psi_s = \int (U_s - I_s R_s) dt. \quad (8)$$

The torque responses of the SPWM- and SVPWM-based DTC schemes for the various speed ranges are shown in Figure 14. The SVPWM improves the torque response prominently for nominal speed range (146.53 rad/s) than SPWM. On the other hand, for medium (58.612 rad/s) and low (8.7918 rad/s) speed

ranges, the torque performance is not satisfactory for SVPWM when compared to SPWM.

In SPWM and SVPWM, the torque error ($T^* - T$) and flux error ($\Psi^* - \Psi$) are given to the PI controllers. The reference torque (T^*) is the output of another PI controller which is taking speed error ($\omega_r^* - \omega_r$) as input. Hence, when the reference speed (ω_r^*) changes to medium and low ranges, the proportionate changes are reflected in the reference signals of the SPWM.

Based on the output of these PI controllers, the reference voltage is calculated for SVPWM [17]. The DC bus voltage (U_{dc}) and the sector angle (α) are used to determine the duty cycles of the voltage vectors. The soft computing controllers are not effective in SPWM as well as SVPWM for the reason that the conventional look-up table as well as the hysteresis comparators is removed. In Figure 15, the reference speed is kept as 146.53 rad/s, and the responses clearly prove that the fuzzy DTC (3fuzzy) which consists of fuzzy-based RFE, fuzzy-based RTE and fuzzy-based sector rotation performs better than other control strategies. The fuzzy-based RFE (1fuzzy) performs better than basic DTC. The fuzzy-based RFE with fuzzy-based RTE (2fuzzy) performs better than fuzzy-based RFE alone.

In Figure 16, the reference speed is reduced to 58.612 rad/s; here also the 3fuzzy DTC and 2fuzzy are

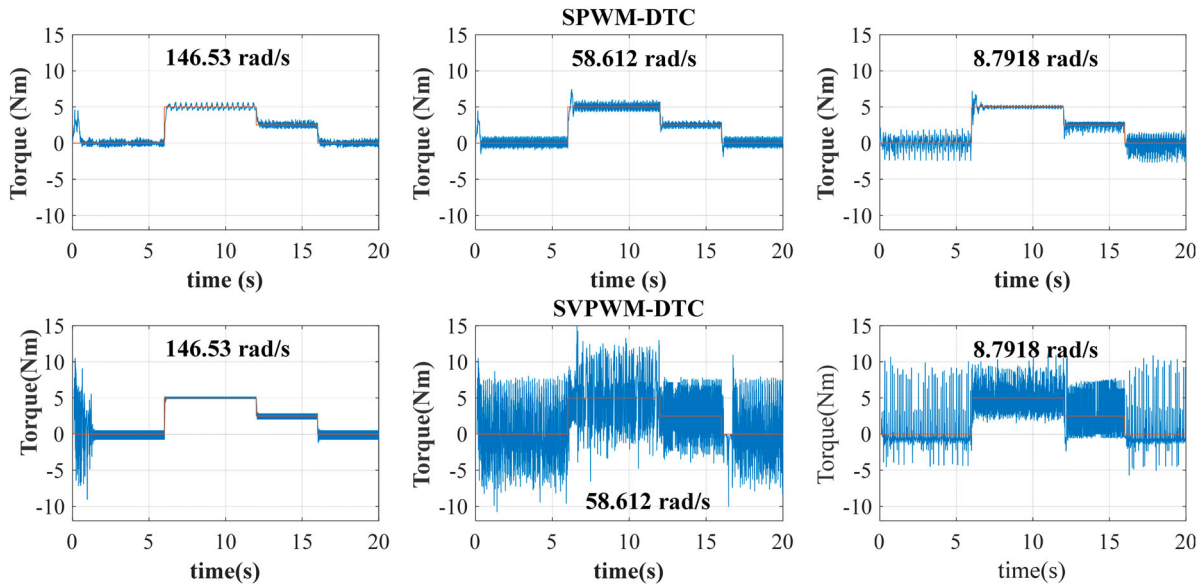


Figure 14. Torque responses of SPWM-DTC and SVPWM-DTC schemes for a speed reference of 146.53, 51.612 and 8.7912 rad/s.

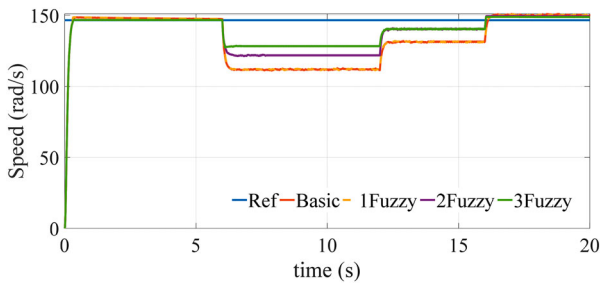


Figure 15. Speed responses of basic, 1fuzzy, 2fuzzy and 3fuzzy DTC schemes for a speed reference of 146.53 rad/s.

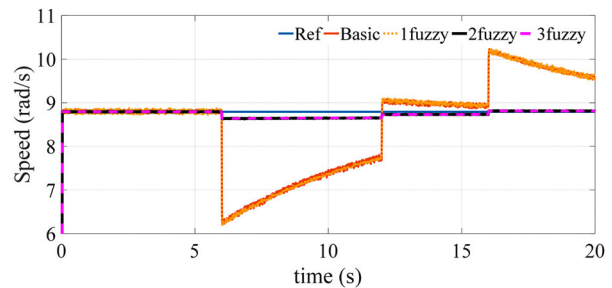


Figure 17. Speed responses of basic, 1fuzzy, 2fuzzy and 3fuzzy DTC schemes for a speed reference of 8.7912 rad/s.

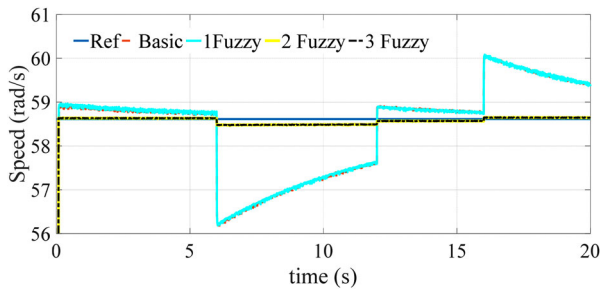


Figure 16. Speed responses of basic, 1fuzzy, 2fuzzy and 3fuzzy DTC schemes for a speed reference of 58.612 rad/s.

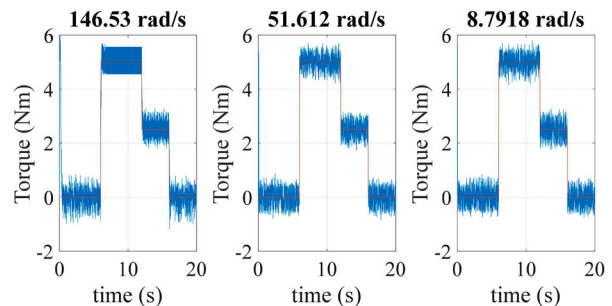


Figure 18. Torque responses of fuzzy DTC (3fuzzy) schemes for a speed reference of 146.53, 51.612 and 8.7912 rad/s.

performing better than basic and 1fuzzy DTC. The responses seem that basic and 1fuzzy are performing same, still the difference can be realized in performance indices in Section 5.4.

Similarly, Figure 17 depicts the speed responses for the reference speed of 8.7912 rad/s. The responses show the similar performance as Figure 16, and the 3fuzzy DTC performs better than other strategies.

From Figures 15–17, it is inferred that the fuzzy DTC (3fuzzy) performs better than other strategies. The torque responses of nominal speed (146.53 rad/s), medium speed (51.612 rad/s) and low speed

(8.7912 rad/s) for fuzzy DTC are shown in Figure 18. The ripples are comparatively less for low speed operating region. During starting time, speed error is equal to reference speed and it approaches to zero at settling time. Hence, speed PI controller output during starting is high (reference torque). It is controlled by adding saturator at the output of the speed PI controller.

5.4. Comparison of performance index

To prove the performance precisely, the proposed fuzzy DTC and basic DTC are compared using the ISE as

Table 5. Performance index ISE for speed and torque error.

Time	Load	Basic DTC		Fuzzy DTC	
		Torque	Speed	Torque	Speed
<i>ISE from simulation</i>					
6–12 s	Full load	966.2472	11,695.06	481.9875	4046.403
12–16 s	Half load	603.156	2913.944	301.9639	1112.417
16–20 s	No load	558.1334	1397.12	276.7639	1193.544
Total		2127.537	16,006.12	1060.715	6352.364
<i>ISE from experimental work</i>					
6–12 s	Full load	860.629	22,025.68	142.364	9414.959
12–16 s	Half load	240.421	5537.231	96.9985	2297.837
16–20 s	No load	168.0812	5989.757	150.0733	2347.524
Total		1269.131	33,552.67	389.4358	14,060.32

performance index.

$$ISE = \int_0^T e(t)^2 dt. \tag{9}$$

The equation for calculating ISE is given in Equation (9), where $e(t)$ represents the error. The performance indices for speed error and torque error are given in Table 5 for basic DTC and fuzzy DTC. The ISE values of fuzzy DTC are less than basic DTC in both simulation and experiment as given in Table 5. In Table 5, the hardware data are taken from DSO as MECSVs file. The same number of data is collected from simulation also to calculate the ISE values.

The bar charts in Figure 19 pictorially represent that the ISE values are low for fuzzy DTC than basic DTC. Hence, it is proved obviously that the fuzzy DTC system improves the torque and speed control better than basic DTC during loading conditions. The system conditions, i.e. IM parameters, PI controller gain values and inverter DC link voltage, are the same under simulation and experimental studies. The responses derived from simulation and experimental studies differ slightly because of FPGA signal processing, direct loading and other real-time variations. By observing the torque response, speed response and performance indices, it is clear that the proposed fuzzy DTC-IM drive gives improved performance than basic DTC-IM drive.

In Table 6, the ISE values of speed error and torque error for various speed ranges as well as for individual control strategies are furnished. It is seen clearly that individual control strategies show the step by step improvement in the speed and torque ISE values. In Table 6, the ISE values are calculated from the Matlab/Simulink[®] directly.

At nominal speed (146.53 rad/s), the torque error ISE value gets reduced by 93.48%. In the same way, for medium and low speed ranges, the torque error ISE value gets reduced by 26.45% and 15.8%, respectively. In the same way, the speed error also gets reduced by 73.26%, 99.47% and 99.36%, respectively, for nominal, medium and low speed ranges. The percentage improvement is calculated by $((4168 - 271.31)/4168) * 100 = 93.48\%$.

Table 6. Performance index ISE for speed and torque error for nominal, medium and low speed ranges.

Reference speed	146.53 rad/s			51.612 rad/s			8.7918 rad/s		
	Basic	Fuzzy flux (1 fuzzy)	With FGS (2 fuzzy)	Basic	Fuzzy flux (1 fuzzy)	With FGS (2 fuzzy)	Basic	Fuzzy flux (1 fuzzy)	With FGS (2 fuzzy)
<i>Torque</i>									
6–12 s (full load)	1357	1354	98.91	1.47	1.2744	1.281	0.6329	0.5353	0.4537
12–16 s (half load)	1218	1219	167.1	0.8212	0.7442	0.6444	0.3862	0.3129	0.3498
16 20 s (no load)	1593	1593	6.833	0.6764	0.6373	0.4918	0.3553	0.2828	0.3537
Total	4168	4166	272.843	2.9676	2.6559	2.4172	1.3744	1.131	1.2589
<i>Speed</i>									
6–12 s (full load)	7075	7012	3598	16.52	16.22	0.1009	18.09	18.43	0.13
12–16 s (half load)	988.5	979	180.5	0.1907	0.1762	0.008	0.1419	0.1735	0.01447
16–20 s (no load)	53.47	50.62	32.73	4.79	4.838	0.004625	4.613	4.644	0.001594
Total	8116.97	8041.62	3811.23	21.5007	21.2342	0.113525	22.8449	23.2475	0.146064

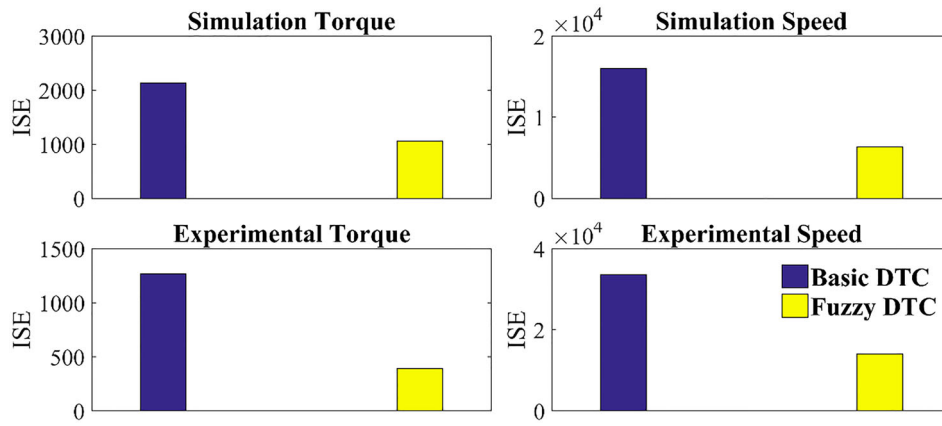


Figure 19. Bar chart representation of the performance index ISE for speed and torque error from simulation and experimental studies.

6. Conclusion

The DTC-IM drive is made highly adaptive by fuzzy logic in this work. Fuzzy logic is used for reference flux estimation, reference torque estimation and sector rotation angle in DTC for performance improvement. The proposed DTC system improves torque and speed response than the basic DTC system. In the proposed system, the reference flux is varied continuously according to system conditions, the FGS is applied for adaptive gain values of the speed PI controller and fuzzy-based sector rotation concept is used for stator flux plot sector division. Furthermore, the proposed DTC-IM drive performance is validated by changing the reference speed to medium and low speed ranges. SPWM-based DTC performs at nominal and medium speed ranges. On the other hand, in low speed range, SPWM is not effective. SVPWM technique gives less torque and speed control at nominal speeds than SPWM for DTC. In medium and low speed ranges, SVPWM is not effective. The comparison with basic DTC clearly proves improvement in system performance with the use of fuzzy logic for the proposed RFE, RTE and sector rotation angle. The experimental results validate the simulation responses and clearly prove the superiority of the proposed system. The performance indices also prove that the proposed fuzzy DTC-IM drive provides a better performance compared to basic DTC-IM drive.

List of symbols

U_{abc}	stator voltages
U_{dc}	DC link voltage
I_{ab}	stator currents
$\alpha[i]$	sector number (i varies from I to VI)
U_{ds}, U_{qs}	stator voltage components of d -axis and q -axis
I_{ds}, I_{qs}	stator current components of d -axis and q -axis
S_a, S_b, S_c	switching states of the inverter

Δt	change in time
$\Delta \Psi$	change in flux
$\Psi_s(\text{old})$	stator flux before applying voltage vector
$\Psi_s(\text{new})$	Stator flux after applying voltage vector
I_s	stator current
U0 to U7	look-up table switching voltage vectors

Disclosure statement

No potential conflict of interest was reported by the author(s).

References

- [1] Bose BK. Modern power electronics and AC drives. New Jersey: Prentice Hall; 2002. 408 p.
- [2] Vas P. Sensor less vector and direct torque control. London: Oxford University Press; 1998. 505 p.
- [3] Stanely HC. An analysis of induction machine. AIEE Trans. 1938;57(Supplement):751–757.
- [4] Wahab HFA, Sanusi H. Simulink model of direct torque control of induction machine. Am J Appl Sci. 2008;5(8):1083–1090.
- [5] Toufouti R, Meziane S, Benalla H. Direct torque control for induction motor using intelligent techniques. J Theor Appl Inform Technol. 2007;3(3):35–44.
- [6] Nasir UM, Muhammad H. FLC-based DTC scheme to improve the dynamic performance of an IM drive. IEEE Trans Ind Appl. 2012;48(2):823–831.
- [7] Jay KP, Mohan VA, Ronak VN, et al. Direct torque control scheme for six-phase induction motor with reduced torque ripple. IEEE Trans Power Electron. 2017;32(9):7118–7129.
- [8] Nikzad MR, Behzad A, Ahmadi SO. Discrete duty cycle method for direct torque control of induction motor drives with model predictive solution. IEEE Trans Power Electron. 2018;33(3):2317–2329.
- [9] Bhoopendra S, Shailendra J, Sanjeet D. Torque ripple reduction technique with improved flux response for a direct torque control induction motor drive. IET Power Electron. 2013;6(2):326–342.
- [10] Kaboli S, Zolghadri MR, Khajeh EV. A fast flux search controller for DTC-based induction motor drives. IEEE Trans Ind Electron. 2007;54(5):2407–2416.
- [11] Faith K, Faruk CM, Yilmaz K, et al. Fuzzy based stator flux optimizer design for direct torque control. Int J Inst Control Syst. 2012;2(4):41–49.

- [12] Sampath KS, Joseph XR, Balamurugan S. Development of ANFIS-based reference flux estimator and FGS-tuned speed PI controller for DTC of induction motor. *Automatika*. 2018;59(1):11–23.
- [13] Bouserhane IK, Hazzab A, Boucheta A, et al. Optimal fuzzy self-tuning of PI controller using genetic algorithm for induction motor speed control. *Int J Autom Technol*. 2008;2(2):85–95.
- [14] Vijaya CKRM, Balamurugan S, Sankaranarayanan K. Variable structure fuzzy gain scheduling based load frequency controller for multi-source multi area hydro thermal system. *Int J Electr Power Energy Syst*. 2013;53:375–381.
- [15] Wong WSH, Holliday D. Minimisation of flux droop in direct torque controlled induction motor drives. *IEE Proc Electr Power Appl*. 2004;151(6):694–703.
- [16] Yuttana K, Suttichi P, Hamid AT. Modified direct torque control method for induction motor drives based on amplitude and angle control of stator flux. *Electr Power Syst Res*. 2008;78(10):1712–1718.
- [17] Buja GS, Marian PK. Direct torque control of PWM inverter-fed AC motors – a survey. *IEEE Trans Ind Electron*. 2004;41(4):744–757.
- [18] Mohamed SZ, Maksoud HA, Shaban MS. Analysis of hysteresis band variations in DTC on the performance of IM drives. *J Electr Syst*. 2020;16(3):350–365.
- [19] Aliaskari A, Zarei B, Davari SA, et al. A modified closed loop voltage model observer based on adaptive direct flux magnitude estimation in sensorless predictive direct voltage control of an induction motor. *IEEE Trans Power Electron*. 2020;35(1):630–638.
- [20] Nikolay D, Hristo M, Julia D. Adaptive controller for induction machine direct torque control. 1-4, July, Bulgaria 17th international conference on electrical machines, drives and power systems (ELMA); 2021.
- [21] Chinthakunta UR, Prabhakar KK, Singh AK, et al. Direct torque control induction motor drive performance evaluation based on torque error status selection methods. *IET Electr Syst Transp*. 2019;9(3):113–127.
- [22] Soukaina ED, Loubna L. Comparison between PI-DTC-SPWM and fuzzy logic for a sensorless asynchronous motor drive. *Protect Control Modern Power Syst*. 2021;6(34):1–13.
- [23] Sayeed M, Malik EE, Donald SZ. PI and estimators for tuning the stator resistance in direct torque control of induction machines. *IEEE Trans Power Electron*. 1998;13(2):279–287.

Appendix

IM parameters

Stator resistance (R_s) = 19.32 Ω , resistance from rotor (R_r) = 8.04 Ω , inductance by mutual (L_m) = 0.601 H, inductance from stator (L_s) = 0.633 H, inductance from rotor (L_r) = 0.633 H, inertia (J) = 0.0051 kg m².

Rated values

Power = 1 HP, voltage (V) = 400 V, speed (ω_r^*) = 146.15 rad/s, torque (T^*) = 5 N m, no of poles (P) = 4.